Max-Planck-Institut
für Meteorologie

REPORT No. 115

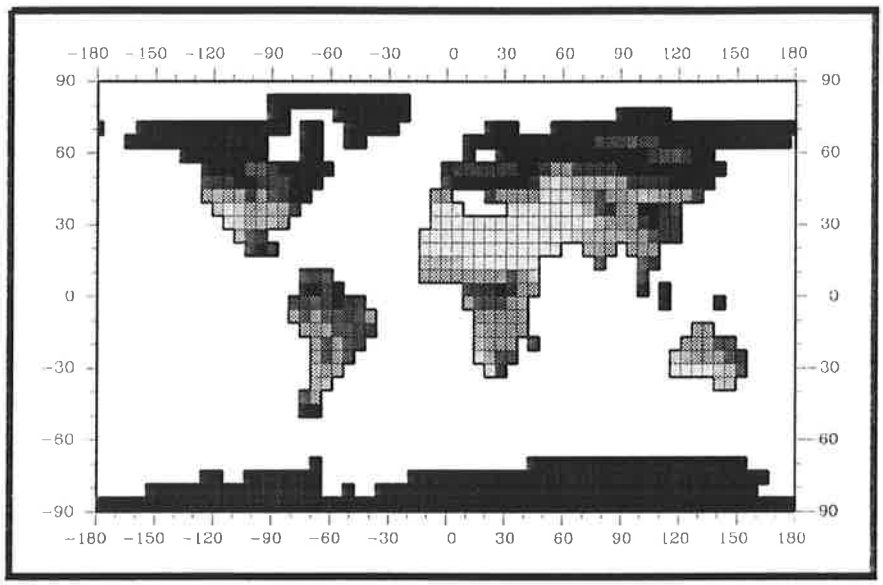

SHIFT OF BIOME PATTERNS DUE TO SIMULATED CLIMATE VARIABILITY AND CLIMATE CHANGE

by

MARTIN CLAUSSEN

HAMBURG, OCTOBER 1993

AUTHOR:

Martin Claussen

Max-Planck-Institut
für Meteorologie

MAX-PLANCK-INSTITUT
FÜR METEOROLOGIE
BUNDESSTRASSE 55
D-20146 Hamburg
F.R. GERMANY

Tel.: +49-(0)40-4 11 73-0
Telex: 211092 mpime d
Telemail: MPI.METEOROLOGY
Telefax: +49-(0)40-4 11 73-298

ISSN 0937–1060

Shift of biome patterns due to simulated climate variability and climate change

Martin Claussen

Max-Planck-Institut für Meteorologie

Bundesstr.55

20146 Hamburg, Fed. Rep. Germany

Abstract

The variability of simulated equilibrium-response patterns of biomes caused by simulated climate variability and climate shift is analysed. This investigation is based on various realisations of simulated present-day climate and climate shift.

It has been found that the difference between biomes computed from three 10-year climatologies and from the corresponding 30-year climatology, simulated by the Hamburg climate model at T21 resolution, amounts to approximately 6% of the total land area, Antarctica excluded. This difference is mainly due to differences in annual moisture availability and winter temperatures. When intercomparing biomes from the 10-year climatologies a 10% difference is seen, but there is no unique difference pattern.

Similar is true when comparing various realisations of present-day and anomaly climate computed from simulations with the same climate model, but at T42 resolution. The interdecadal variation of biome patterns due to interdecadal climate variability varies between 8-12%. Again, there is no unique difference pattern, and differences in biomes are mainly induced by changes in annual moisture availability, i.e. by variations in the simulated hydrological cycle. The variability of temperature plays only a secondary rôle. Comparing biomes deduced from a single-year and a 10-year integration yield a difference of almost 25%.

In contrast to the interdecadal variability, the shift of conditions favorable for biomes due to a shift in climate in the next 100 years, caused by an increase in sea-surface temperatures and atmospheric CO_2, reveals a unique trend pattern. It turns out that the strongest and most significant signal is the north-east shift of conditions for boreal biomes. This signal is caused by an increase of annual temperature sums as well as mean temperatures of the coldest and warmest months. Trends in annual moisture availability are of secondary importance globally. Regionally, a decrease in water availability affects biomes in Central and East Europe and an increase of water availability leads to a potential increase in tropical rain forest. In total, all differences amount to roughly 30% of the total land surface, Antarctica excluded.

1 Introduction

The climate system consists of several subsystems which interact in a complex, nonlinear way at a wide range of time scales. The interaction between atmosphere and ocean has been simulated during the last few years (e.g. Cubasch et al. 1992). Less attention has been paid to the interactive integration of biosphere and atmosphere although the sensitivity of climate simulations to changes in vegetation patterns is well documented (e.g. Mintz, 1984).

Only recently, global vegetation patterns have been computed from simulated climatology (e.g. Prentice and Fung, 1990, Claussen and Esch, 1993, Henderson-Sellers, 1993). And perhaps the first attempt to incorporate continental vegetation as a dynamic component of a global climate model has been undertaken by Henderson-Sellers (1993). In these studies, the vegetation models are static, equilibrium-response models. Henderson-Sellers (1993) uses a simplified Holdrige scheme, and Claussen and Esch, Prentice et al. (1992) biome model.

Here, also Prentice's et al. (1992) model of biomes, i.e. potential natural vegetation zones, is chosen, because this model is based on physiological considerations rather than on correlations between climate distribution and biomes as they exist today. Biomes are not taken as given as, for instance, in the Holdrige classification, but emerge through the interaction of constituent plants. Hence the biome model can be applied to the assessment of changes in natural vegetation patterns in response to changes in climate. However, it is important to notice that the biome model does not simulate the transient dynamics of vegetation. At best, it provides constraints within which plant community dynamics should operate. In this sense, *shift of biome patterns* has to be taken as *shift of conditions favorable for biomes* in the following.

When estimating global patterns of biomes from a simulated climatology the question arises what the appropriate time span is over which the climatology has to be evaluated. Or the other way round, how strong differ the global patterns of biomes when computed from a 10-year climatology and from a 30-year climatology? Since a climate model simulates a chaotic system, various realisations of the same climate generally differ. The shorter the integration interval, the larger the differences amongst various realisations. Hence from a modellers point of view it is necessary to know the response of the biome

model to the simulated climate variability. (Of course, similar ideas apply also to natural climate variability.) An associate problem is the detection of a significant signal of global shifts of biomes due to simulated climate changes.

Therefore, the problem of the sensitivity of a biome model to simulated climate variability is addressed by analysing several numerical realisations of present-day climate and of climate anomalies induced by enhanced sea-surface temperatures and atmospheric CO_2 concentrations. Also, the dependence of biome variability on the resolution of the climate model is outlined (Section 3). By comparing biomes computed from simulated present-day climates and anomaly climates, the shift of biomes due to a climate trend is estimated in terms of its structure and significance (Section 4). Before discussing the analyses, the climate model and the biome model used here are briefly presented (Section2).

2 Climate model and biome model

2.1 The climate model

Results of climate simulations are taken from the climate model developed at the Max-Planck-Institut in Hamburg. The model physics as well as its validation is described in detail by Roeckner et al. 1992.

Currently, there are no specific biomes or vegetation types prescribed in the climate model. Instead, a vegetation ratio is assigned to each grid box using data of Wilson and Henderson-Sellers (1985), albedo is derived from satellite data of Geleyn and Preuss (1983), and roughness length is computed from the variance of orography (Tibaldi and Geleyn, 1981) and a vegetation roughness length evaluated by Baumgartner et al. (1977). The leaf area index and minimum stomatal resistance are global constants. Despite these rather crude representation of vegetation in the climate model, the global patterns of biomes computed from its climatology agree quite well with those computed from the IIASA (International Institute of Applied Systems Analysis) climate data (Claussen and Esch, 1993) using Prentice et al.(1992) biome model.

2.2 The biome model

In the biome model of Prentice et al. (1992) 14 plant functional types are assigned climate tolerances in terms of amplitude and seasonality of climate variables (see Table 1). Table 1 is largely empty, because climate tolerances are not specified without a known or hypothesized mechanism.

The cold tolerance of plants is expressed in terms of minimum mean temperature of the coldest month. Some plant types also have chilling requirements expressed in terms of a maximum mean temperature of the coldest month.

The heat requirement of plant types is given in terms of annual accumulated temperatures over 5°C, for some plant types a threshold of 0°C is used. The heat requirement of some shrub types is given by the mean temperature of the warmest month.

The third basic climate tolerance is associated with moisture requirement in terms of annual moisture availability. All plant types, except for desert shrub, have minimum tolerable values of annual moisture availability. Only tropical raingreen also has an maximum tolerable value. The annual moisture availability is defined as ratio of actual evapotranspiration (AET) and potential evapotranspiration (PET). PET basically depends on net-radiation, i.e. solar radiative input, radiative cooling, and cloudiness. AET, in addition, requires prescription of precipitation and soil water capacity. Hence for evaluation of annual moisture availability, monthly means of temperature, precipitation, cloudiness, and information on soil water capacity are needed as input variables. (Actually the biome model uses sunshine in terms of percentages of possible hours of bright sunshine, i.e. an inverse measure of cloudiness.)

The biome model predicts which plant functional type can occur in a given environment, i.e. in a given set of climate variables. Then the biome model selects the potentially dominant plant types according to the dominance hierarchy. Finally, biomes are defined as combinations of dominant types. The dominance hierarchy is an artificial device whose main purpose is to facilitate comparison with the global vegetation classification of Olson et al. (1983). In Table 2, the allocation of plant functional types to biomes is summarized.

A potential weakness of the biome model is that CO_2 effects on vegetation are not

considered. It has been found that rising CO_2 in the atmosphere accelerates net primary productivity and probably increases carbon storage in biomes. The accretion of carbon by natural ecosystems could account for the so-called missing carbon sink. On the other hand, the strength of global CO_2 fertilization as function of nutrient and hydrological cycles is poorly known (e.g. Wisniewski and Lugo, 1992).

Prentice et al. (1992) have use the IIASA climate data base, described by Leemans and Cramer (1990), and soil texture data (to estimate soil water capacity) from the FAO soils map (FAO, 1974). Their predictions of global patterns of biomes are in good agreement with the global distribution of actual ecosystem complexes being evaluated by Olson et al. (1983). Where intensive agriculture has obliterated the natural vegetation, comparison of predicted biomes and observed ecosystems is, of course, omitted.

It is important to notice that the biome model is an equilibrium-response model; it does not simulate the transient dynamics of vegetation. By assuming a unique relation between plant physiology and climate the biome model could, at best, provide a global-scale constraint within which plant community dynamics should operate. Hence whenever *biome variability* or *shift of biomes* is mentioned in the following, it is to be understood as *variability of conditions favorable for biomes* or *shift of conditions favorable for biomes*.

3 Shift of biomes due to climate variability

3.1 Simulation of present-day climate at T21 resolution

Biomes are computed using model results of three 10-year integrations performed with the climate model at T21 resolution (5.6° × 5.6°, i.e. appr. 600 km × 600km at the equator) undertaken at the Max-Planck Insitut für Meteorologie, Hamburg. Each simulation is forced by the same boundary data, in particular, by the same climatology of the annual cycle of SST (sea-surface temperatures) averaged for the years 1979 to 1988. Only the initial values differ. These data set are called T21C1, T21C2, T21C3. A fourth data set, T21C0, is generated by averaging the three 10-year integrations to get a 30-year climatology.

The biomes computed from T21C0-3 are depicted in Figures 2 - 5 (for allocation of colors to biomes, see Figure 1). At the first glance, there are no major differences. When comparing biomes estimated from each 10-year integrations and from the 30-year average, only approximately 6 % of the land surface (excluding Antarctica) are occupied by different biomes. When intercomparing biomes evaluated from all 10-year integrations the difference amounts to roughly 10%. Of course, the interdecadal variation of climate is larger than the difference between a 10-year and the 30-year average. Hence one obtains a reasonable guess of global patterns of biomes when using 10-year climatology instead of a 30-year climatology.

Where do the differences in biomes computed from runs T21C0-3 originate from? Table 3 lists the percentage of land area (excluding Antarctica) taken by each biome (columns 1 to 4). Column 5 shows the standard deviation of biomes from runs T21C1 - 3. This standard deviation can be viewed as variability of biomes due to (simulated) interdecadal climate variability. Column 6 gives the difference between the arithmetic average of columns 2,3,4 and column 1. This difference clearly demonstrate that the global patterns of biomes estimated form a 30-year climatology does not coincide with an 'average' pattern of biomes estimated from the three 10-year climatologies taken from the corresponding 30-year period. This is not exspected because the relationship between biomes and climate is highly non-linear. Finally, columns 7 lists the ratio of column 6 and 5. This value can be interpreted as a measure of physical significance or consistency of differences between biomes computed from the three 10-year climatologies and the 30-year climatology. It is readily seen that the largest difference between biome patterns is due to changes in biome 5, i.e. temperate deciduous forest, but the most consistent difference is due to changes in biome 6, i.e. cool mixed forest.

Trend matrices yield further details. In Table 4, the trends between biomes computed from T21C1 and T21C0 are listed. The matrix has to be interpreted in the following way. A value y_{ij} in line i and row j indicates that y% of the total land area (Antarctica excluded) which are covered by biome i in T21C0 are covered by biome j in T21C1. For example, cool mixed forest (biome 6) found in T21C0 are replaced by temperate deciduous forest (biome 5) in T21C1, and this change occupies 0.57% of the total land area. Likewise, cool grass/shrub (biome 13) found in T21C0 is temperate deciduous

forest (biome 5) in T21C1, again, for 0.57% of the total land surface. The change from cool mixed forest to temperate deciduous forest is large also in the other two trend matrices T21C2 - T21C0 and T21C3 - T21C0 (not shown here). Hence the most consistent difference between biomes computed from T21C1-C3 and from T21C0 is due to a change from biome 6 (in T21C0) to biome 5 (in T21C1-C3). On the other hand, the strongest differences between biomes computed from runs T21C1-C3 and from run T21C0 originates from differences in temperate deciduous forest (biome 5). The trend matrix T21C1-T21C0 reveals that this is due to changes between cool mixed forest (biome 6) *and* cool grass/shrub (biome 13) to temperate deciduous forest (biome 5). This is supported by trend matrices T21C2-T21C0 and T21C3-T21C0 which also indicate changes from warm temperate forest (biome 4) and warm grass/shrub (biome 12) to tempearature deciduous forest. On average, climate model data T21C1-C3 yield less cool mixed forest and more temperate deciduous forest than T21C0 (see also Table 3).

The shift of biomes can be attributed to differences in climate tolerances between runs T21C0 - 3. From Table 1, it is seen that temperate deciduous forest and cool mixed forest differ by the plant functional type boreal evergreen conifer. By comparing climate tolerance of temperate summergreen, cool-temperate conifer, boreal summergreen, and boreal evergreen conifer (see Table 1) it is obvious that boreal evergreen conifer vanishes, if the annual moisture availability becomes too small, i.e. $0.65 < \alpha < 0.75$, or if the winter becomes too warm such that the temperature of the coldest month exceeds -2°C. Global distributions of annual moisture availability (Figures 6, 7) and mean temperature of the coldest month (Figures 8, 9) reveal that in East Europe and North America, where changes from temperate deciduous forest to cool mixed forest occur (compare Figures 2 - 5), the annual moisture availability exceeds 0.9, but the temperature of the coldest month is below -2°C in the data of T21C0 and above, in T21C1. The same is valid also for T21C2 and T21C3. Hence the most consistent difference between biomes computed from T21C0 and T21C1-C3 is due to a variability of winter temperatures.

Following a similar reasoning, it can be demonstrated that changes between cool or warm grass/shrub and temperate deciduous forest are due to variability of annual moisture availability, and changes between warm temperate forest and temperate deciduous for-

est, again, due to winter temperatures. Hence the strongest difference between biomes computed from the 30-year climatology and from the 10-year climatologies is caused by both, variability of winter temperatures as well as annual moisture availability.

Trend matrices of biomes amongst the three 10-year integrations only have also been evaluated, but are not listed here. It turns out that these three trend matrices have no common structure, except that in two cases the conversion from hot desert (biome 15) to warm grass/shrub (biome 12) is strongest. In the third case, the change from temperate deciduous forest (biome 5) to cool mixed forest (biome 6) dominates. When interpreting these changes in terms of variations of climate tolerances (see Table 1), it emerges that the strongest changes are due to interdecadal changes in annual moisture availability and winter temperatures, as seen in the differences between biomes from 10-year and the 30-year climatology.

3.2 Comparison of a 10-year and a single year integration at T42 resolution

A 10-year integration and a single year integration using the climate model at T42 resolution (2.8125° × 2.8125°, i.e. appr. 300 km × 300km at the equator), both performed at the Max-Planck Institut für Meteorologie, Hamburg, are analysed in terms of biomes. This exercise is undertaken to explore the difference in global patterns of biomes if biomes are estimated from a single year climatology instead of a 10-year climatology. It is motivated by recent studies of Henderson-Sellers (1993) who coupled a simplified Holdrige vegetation scheme to a climate model by feeding the information of the vegetation model to the climate model at the end of each year. Hence it should be worthwhile to ask how representative a global distribution of biomes computed from just one year of model data is.

By comparing biomes estimated from both integrations it can be found that nearly a quarter (24.4%) of the total land area (Antarctica excluded) is covered by different biomes. This is quite strong a change, in its magnitude almost as large as a shift of biomes due to a change in climate discussed in section 4.

The trend matrix, called V10-V1 and given in Table 5, reveals some details. the strongest difference is seen in savanna (biome 3) and tropical seasonal forest (biome 2). Approximately 2.8% of the total land area which is covered by savanna in the single year integration is covered by tropical seasonal forest in the 10-year integration. The second largest shift is from xerophytic woods/shrub (biome 11) to savanna ($\sim$ 2.5%), followed by a change from hot desert (biome 15) to warm grass/shrub (biome 12) ($\sim$ 1.6%).

In terms of climate tolerances, the above mentioned differences are mainly caused by differences in the annual moisture availability as can be deduced from Table 1. Only for the change from xerophytic woods/shrub to warm grass/shrub, an increase in winter temperatures can also be responsible.

3.3 Comparison of present-day and anomaly climate simulations

Biomes are computed from three realisations of present-day climate simulations (in the following called control runs) using 10-year integrations by the climate model T42 resolution. The boundary conditions are interpolated from the same SST data as used for the climate simulations at T21 resolution analysed in the previous section. Again, the boundary conditions of the three realisations are identical, only the initial conditions differ.

The same is done for three 10-year integrations of anomaly climate performed by Perlwitz (1992) (called anomaly runs). As boundary conditions, Perlwitz took observed climatological SST data (the period 1979-1988) and superimposed the SST change obtained from the last 10 years of a transient 100-year integration with the coupled ocean/atmosphere general circulation model (Cubasch et al. 1992). For the latter, the CO_2 increase was prescribed according to the Intergovernmental Panel on Climate Change (IPCC) Scenario A. In the last 10 years, the average amount of CO_2 was set to 1145 ppm, and the global mean near surface temperature is approximately 2.4 °C higher than today. As examples, biomes computed from one of the control and one of the anomaly runs are shown in Figures 10 and 11.

Trend matrices have been computed to investigate the differences of biomes amongst

the control runs and anomaly runs, respectively. Generally, 9% – 12% of the total land area (Antarctica excluded) are involved in any change of biomes - roughly the same number found for the variability of biomes from the 10-year integrations at T21 resolution. Again, no common, unique structure of trend matrices is found, except that in three out of six cases (three control and three anomaly runs), the conversion from hot desert (biome 15) to warm grass/shrub (biome 12) is strongest and in two cases, savanna (biome 3) to tropical seasonal forest (biome 2). The second largest signal are caused by changes from warm grass/shrub to xerophytic woods/shrub (biome 11). As an example, the trend matrix C2-C1 in which biomes from two control runs are compared is given in Table 6. These changes are basically due to a variability of annual moisture availability. The difference between warm grass/shrub and xerophytic woods/shrub could also be caused by an increase in winter temperatures (see Table 1). Therefore, when computing biomes from 10-year climate simulations, the interdecadal variability of water availability, i.e. the hydrological cycle, causes the strongest differences.

4 Assessment of climate change

In the following, the biomes computed from the control runs and anomaly runs at T42 resolution are compared. Assuming that the control runs and the anomaly runs, respectively, are statistically independent, it seems worthwhile to compare biomes computed from each control run with those from each anomaly run, hence nine trend matrices can be set up. These matrices should be viewed upon as means of assessing climate change, not really vegetation change. At best, they provide constraints within which plant community dynamics will operate. As mentioned earlier, the biome model itself is not capable of simulating any rapid change of biomes.

In contrast to the results of the previous section, the new trend matrices resemble each other. As example, the matrix S2-C2 is given as Table 7. All trend matrices show a strong change from tundra (biome 14) to taiga (biome 8), in range of 3.5% – 3.8% of total land area (Antarctica excluded), followed by changes from taiga to cool conifer forest (biome 7), 2.1% – 3.1%, and from cool conifer forest to cool mixed forest (biome 6), 1.3% – 1.9%. Furthermore, there is always a change from polar desert (biome 17)

to tundra (biome 14). All changes in biomes cover approximately 30% of the total land surface, i.e. the shift of biomes due to a climate change is approximately three times larger than that due to interdecadal climate variability.

In Table 8, the land area covered by each biome computed from the three control runs and from the three anomaly runs are listed in columns 1-3 and 4-6, respectively. Columns 7 and 8 list the standard deviations s_c and s_s among biomes from the control runs and anomaly runs, respectively. Column 9 presents the difference between averages of three control runs and of three anomaly runs, $\overline{s} - \overline{c}$. The last column depicts a crude measure of a signal-to-noise ratio t. According to the t-test, t is computed as

$$t = \sqrt{n} \frac{\overline{s} - \overline{c}}{\sqrt{s_s^2 + s_c^2}} \quad ,$$

where n is the number to samples, here $n = 3$. The hypothesis $\overline{s} = \overline{c}$ can be rejected at 1% (5%) significance level, if $t > 4.6(2.78)$ or $t < -4.6(-2.78)$.

It is obvious that the change in tundra (biome 14) is not only the largest, but also the most significant one. The trend matrix S2-C2, furthermore, indicates that this change is mainly due to a conversion from tundra (in the control run) to taiga (in the anomaly run). Changes from tundra to cold mixed forest (biome 10), to cool grass/shrub (biome 13), and to cool desert (biome 16) as well as the conversion from polar desert (biome 17) to tundra are only of secondary importance, although the latter conversion is quite significant. By contrast, changes in savanna (biome 3) and tropical seasonal forest (biome 2) are as large or even larger than changes in cool desert (biome 16) and polar desert (biome 17), but the latter are significant, the former, not at all.

When inspecting the global distribution of climate parameters (not shown here), the following conclusions can be drawn. The change from tundra to taiga is associated with a change of plant types from cold grass/shrub to boreal evergreen conifer and boreal summergreen These plant types differ by their drought tolerance, i.e. minimum annual moisture availability, and heat requirement, i.e. growing degree-days. Since the annual moisture availability is always large at high latitudes, it is the growing degree-days on 5°C base which affects the northern limit of boreal evergreen conifer and boreal summergreen. Hence the increase of annually integrated temperatures causes the northward shift of taiga at the expense of tundra. Similar is valid for the change from

polar desert to tundra, the latter biome being limited by the growing degree-days on 0°C base. Also the strong, and still significant, shift from taiga to cool conifer forest and from cool conifer forest to cool mixed forest is caused by an increase in growing degree-days. Changes from cool grass/shrub (biome 13) to warm grass/shrub (biome 12) as seen in the Rochy Mountains and in Manchuria (compare Figures 10, 11) can be traced back to an increase in summer temperatures. There, the mean temperature of the warmest month exceeds 22°C. Similar is true for the conversion from cool desert (biome 16) to hot desert (biome 15), a rather small, but significant signal, seen in the Taklimakan region and at the northern coast of Chile. The change from warm grass/shrub (biome 12) to xerophytic woods/shrub (biome 11), as consistenly seen in south-western Europe, is due to an increase of winter temperatures.

Changes in annual moisture availability are responsible for a shift of biomes in central and eastern Europe where the annual moisture availability is smaller (by -0.25) in the anomaly runs. As a consequence, warm grass/shrub is seen instead of temperate deciduous forest and cool mixed forest (compare Figures 10, 11). Moreover, there are parts in East Europe, where winter temperatures are sufficiently small to sustain boreal evergreen conifer but the annual moisture availability is below 0.75. A rather large and significant change in biomes, caused by an increase in annual moisture availability above 0.95, is noticable mainly in the Congo and in the Amazonian region where the climate conditions become favorable for tropical rain forest (biome 1) instead for tropical seasonal forest (biome 2).

Overall, the shift of biomes due to a climate change is caused mainly by changes in temperature in the first place, while changes in the hydrological cycle, i.e. in the annual moisture availability, play only a secondary rôle. This is at variance with results from previous section which indicate that interdecadal variability of annual moisture avalability is responsible for most of the changes in biomes.

5 Conclusion

The variability and the shift of biomes due to simulated climate variability and climate change has been addressed by analysing various realisations of simulated present-day climate and anomaly climate, the latter induced by an increase in SST and atmospheric CO_2 concentration. For the anomaly integrations, boundary values are taken from the last ten years of a transient 100-year integration, where the CO_2 increase is prescribed according to the IPCC Scenario A (for details see Cubasch et al., 1992). Biomes have been computed using the biome model of Prentice et al. (1992). This model is a static, equilibrium-response model, hence its results can be interpreted at best as constraints within which plant community dynamics could operate. The terms *variability and shift of biomes* are really to be taken as *variability and shift of conditions favorable for biomes.*

It has been found that the difference between biomes computed from three 10-year climatologies and from the corresponding 30-year climatology amounts to approximately 6% of the total land area, Antarctica excluded. This difference is mainly due to differences in annual moisture availability and winter temperatures. Intercomparing biomes from the 10-year climatologies a 10% difference is seen, but there is no unique difference pattern. These results are obtained by using climatologies simulated at T21 resolution.

Similar is valid when comparing various realisations of present-day and anomaly climate computed at T42 resolution. The interdecadal variability of biomes due to interdecadal climate variability varies in between 8-12%. Again, there is no unique difference pattern, and differences in biome are mainly induced by changes in annual moisture availability, i.e. by the interdecadal variability of the simulated hydrological cycle. The variability of the temperatue signal plays only a secondary rôle. Comparing biomes deduced from a single-year and a 10-year integration yields a difference of almost 25%.

In contrast to the interdecadal variability, the shift of biomes due to a shift in climate reveals a unique trend pattern. The climate anomalies were induced by an increase of atmospheric CO_2 to 1145 ppm leading to a near surface warming of 2.4°C globally. When comparing differences in biome patterns estimated from each realisation of the present-day climate and each of the anomaly climate it turns out that the strongest and most significant signal is the north-east shift of boreal biomes. This signal is caused by an increase of annual temperature sums as well as mean temperatures of the coldest and

warmest months. Trends in annual moisture availability are of secondary importance globally. Regionally, a decrease in water availability is responsible for shift of cool mixed forest in Central and East Europe and an increase of water availability, for an increase in tropical rain forest. In total, all differences amount to roughly 30% of the total land surface, Antarctica excluded.

From these results the following conclusions concerning climate and biome modelling can be drawn. Biomes estimated from a single-year climatology are a rather random product. Differences between biome patterns from a single-year and a 10-year climatology are almost as large as induced by a major climate change considering both, the total change and changes in single biomes. For example, the distribution of biomes from the single-year climatology (not shown here) accidently resemble that from the anomaly climate. Presumably, the interannual variability of biomes computed from various single-year climatologies is also as large as 30%. Henderson-Sellers (1993) reports of smaller interannual percentage changes of some 10%. It should be interesting to check whether this discrepancy is due to different climate variabilities simulated by different climate models or due to use of different vegetation prediction schemes.

By contrast, biome patterns estimated from a 10-year climatology are rather close to those evaluated from a 30-year climatology. Hence a 10-year climatology seems to be a minimum requirement, if one would like to estimate a global pattern of biomes close to a long-term equilibrium. As a consequence, it does not seem advisable to couple the biome model of Prentice et al. (1992) to the Hamburg climate model by computing new patterns of biomes at the end of each year and feeding this new surface information into the climate model - as done by Henderson-Sellers (1993) with their model components. However this problem will be subject to a subsequent study in progress.

It is understood that studying the (numerical) variability of biome patterns due to simulated climate variability is a prerequisite to assessing shifts of biomes due to climate changes. It is possible that a shift in biomes is large, but statistically insignificant. For example, in this study it is found that changes in savanna and tropical seasonal forest are as large or even larger than changes in hot desert and polar desert, however, the latter are quite significant, the former, not at all. The reason for this is the strong sensitivity of savanna and tropical seasonal forest to interdecadal variations in the climate model.

Of course, the variability of biome patterns due to simulated climate variability is a numerical artifact. Perhaps the decay of natural biomes may occur rather rapidly, but the growth of new ones is associated with larger time scales. Currently, only plant community dynamics models (PCM) are able to assess the problem of succession, but they operate at very fine scales of some 30 m $\times$ 30 m. Perhaps, combination of PCM with global terrestrial biogeochemical models can bridge the scale problem. Meanwhile, one has to live with static biome models which necessitates studies like the present one.

Acknowledgements

The authors would like to thank Colin Prentice, Dept. of Plant Ecology, Lund University, Sweden, for making the biome model available. Thanks are also due to Jan Perlwitz, Universität Hamburg, for model data of the anomaly experiment. The author appreciates helpful suggestions by Lennart Bengtsson and Martin Heimann, both at Max-Planck-Institut für Meteorologie.

References

Baumgartner A, Mayer H and Metz W (1977) Weltweite Verteilung des Rauhigkeitsparameters z_0 mit Anwendung auf die Energiedissipation an der Erdoberfläche. Meteorolog.Rdsch. 30: 43-48.

Claussen M and Esch M (1993) Biomes computed from simulated climatologies. Climate Dyn. (in press) also available as Report 89, Max-Planck-Institut für Meteorologie, Hamburg.

Cubasch U, Hasselmann K, Höck H, Maier-Reimer E, Mikolajewicz U, Santer BD, Sausen, R (1992) Time -dependent greenhouse warming computations with a coupled ocean-atmosphere model. Climate Dyn. 8: 55-69.

FAO/UNESCO (1974) Soil map of the world 1:5,000,000. FAO, Paris.

Geleyn J-F and Preuss HJ (1983) A new dataset of sattelite-derived surface albedo values for operational use at ECMWF. Arch.Meteor.Geophys.Bioclim., Ser.A 32: 353-359.

Henderson-Sellers A (1993) Continental vegetation as a dynamic component of global climate model: a preliminary assessment. Climatic Change 23: 337-378

Leemans R and Cramer W (1991) The IIASA database for mean monthly values of temperature, precipitation, and cloudiness on a global terrestrial grid. IIASA Research Report RR-91-18, Laxenburg, Austria.

Mintz Y (1984) The sensitivity of numerically simulated climates to land-surface boundary conditions. in: Houghton J The global climate. Cambridge Univ. Press.

Olson JS, Watts JA, Allison LJ (1983) Carbon in live vegetation of major world ecosystems. ORNL-5862, Oak Ridge National Laboratory, Oak Ridge.

Perlwitz J (1992) Preliminary results of a global SST anomaly experiment with a T42 GCM. Annales Geophysicae Abstracts of the VII General Assembly of the European Geophysical Society in Edinburgh, Apr. 6-10, 1992.

Prentice IC, Cramer W, Harrison SP, Leemans R, Monserud RA, and Solomon AM (1992) A global biome model based on plant physiology and dominance, soil properties and climate. Journal of Biogeography 19: 117-134.

Prentice KC, Fung IZ (1990) The sensitivity of terrestrial carbon storage to climate change. Nature 346: 48-51.

Roeckner E, Arpe K, Bengtsson L, Brinkop S, Dümenil L, Kirk E, Lunkeit F, Esch M, Ponater M, Rockel B, Sausen R, Schlese U, Schubert S, Windelband M (1992) Simulation of the present-day climate with the ECHAM model: Impact of model physics and resolution. Report 93, Max-Planck-Institut für Meteorologie, Hamburg.

Tibaldi S and Geleyn J-F (1981) The production of a new orography, land-sea mask and associated climatological surface fields for operational purposes. ECMWF Tech.Memo. 40.

Wilson MF and Henderson-Sellers A (1985) A global archive of land cover and soils data for use in general circulation climate models. Journal of Climatology 5: 119-143.

Wisniewski J and Lugo AE (1992) Natural Sinks of CO_2. Kluwer Academic Publishers, Dordrecht.

Table 1: Climate tolerances for plant functional types used in the biome model. $T_{c,i}, T_{c,a}$: minimum and maximum tolarable mean temperature of the coldest month, gdd5: minimum growing degree-days on 5°C base, gdd0, on 0°C base, T_w minimum tolerable mean temperature of the warmest month, $\alpha_{i,a}$: minimum and maximum tolerable annual moisture availability, D: dominance hierarchy.

	$T_{c,i}$	$T_{c,a}$	gdd5	gdd0	T_w	α_i	α_a	D
Trees								
tropical evergreen	15.5					0.80		1
tropical raingreen	15.5					0.45	0.95	1
warm-temperate evergreen	5					0.65		2
temperate summergreen	-15	15.5	1200			0.65		3
cool-temperate conifer	-19	5	900			0.65		3
boreal evergreen conifer	-35	-2	350			0.75		3
boreal summergreen		5	350			0.65		3
Non-trees								
xerophytic woods/shrub	5					0.28		4
warm grass/shrub					22	0.18		5
cool grass/shrub			500			0.33		6
cold grass/shrub				100		0.33		6
hot desert shrub					22			7
cool desert shrub				100				8
polar desert								9

Table 2: Allocation of plant types to biomes in Prentice's et al. (1992) biome model.

Plant types	no.	Biome name
tropical evergreen =	01	tropical rain forest
tropical evergreen +		
tropical raingreen =	02	tropical seasonal forest
tropical raingreen =	03	savanna
warm-temperate evergreen =	04	warm mixed forest
temperate summergreen +		
cool-temperate conifer +		
boreal summergreen =	05	temperate deciduous forest
temperate summergreen +		
cool-temperate conifer +		
boreal evergreen conifer +		
boreal summergreen =	06	cool mixed forest
cool-temperate conifer +		
boreal evergreen conifer +		
boreal summergreen =	07	cool conifer forest
boreal evergreen conifer +		
boreal summergreen =	08	taiga
cool-temperate conifer +		
boreal summergreen =	09	cold mixed forest
boreal summergreen =	10	cold deciduous forest
xerophytic woods / shrub =	11	xerophytic woods / shrub
warm grass / shrub =	12	warm grass / shrub
cool grass / shrub +		
cold grass / shrub =	13	cool grass / shrub
cold grass / shrub =	14	tundra
hot desert shrub =	15	hot desert
cool desert shrub =	16	cool desert
polar desert =	17	ice / polar desert

Table 3: Percentage land area (Antartica excluded) taken by each biome (for numbers see Table 2) computed from climate runs T21C0 - 3 (columns 1 - 4). Standard deviation of biomes from runs T21C1 - 3 (column 5). Difference between biomes from T21C0 and average from T21C1 - 3 (column 6). Level of physical significance of differences between previous averages(column 7).

01	2.78	3.05	3.33	2.78	0.27	0.27	0.99
02	4.13	3.59	3.85	4.41	0.42	-0.18	0.43
03	17.26	17.27	16.71	16.47	0.41	-0.45	1.10
04	3.11	3.44	2.95	2.89	0.30	-0.01	0.04
05	2.92	3.85	3.36	3.80	0.27	0.75	2.75
06	4.01	3.79	3.80	3.76	0.02	-0.23	10.51
07	2.39	1.86	2.17	1.97	0.16	-0.39	2.45
08	9.31	9.79	9.70	8.93	0.47	0.17	0.36
09	0.53	0.35	0.71	0.96	0.30	0.14	0.47
10	0.77	0.33	0.64	0.91	0.29	-0.15	0.51
11	9.76	9.43	10.01	10.31	0.45	0.16	0.35
12	5.51	5.56	4.57	5.61	0.59	-0.26	0.45
13	3.74	3.81	3.56	3.11	0.35	-0.25	0.69
14	10.87	11.11	10.79	11.28	0.25	0.19	0.76
15	17.30	17.52	18.03	17.34	0.36	0.33	0.92
16	0.69	0.45	0.69	0.89	0.22	-0.02	0.07
17	10.34	10.23	10.55	10.02	0.27	-0.07	0.26

Table 4: Trend matrix T21C1-T21C0 (for explanation, see text, section 3.1)

	01	02	03	04	05	06	07	08	09	10	11	12	13	14	15	16	17
01	0	0	0	0	0	0	0	0	0	0	0	0	0	0	0	0	0
02	.26	0	.27	0	0	0	0	0	0	0	0	0	0	0	0	0	0
03	0	0	0	0	0	0	0	0	0	0	.27	0	0	0	0	0	0
04	0	0	0	0	0	0	0	0	0	0	.19	0	0	0	0	0	0
05	0	0	0	0	0	0	0	0	0	0	0	.21	0	0	0	0	0
06	0	0	0	0	.57	0	0	0	0	0	0	0	0	0	0	0	0
07	0	0	0	0	0	.35	0	.17	0	0	0	0	0	0	0	0	0
08	0	0	0	0	0	0	0	0	0	0	0	0	0	0	0	0	0
09	0	0	0	0	0	0	0	0	0	0	0	0	.17	0	0	0	0
10	0	0	0	0	0	0	0	.15	0	0	0	0	0	.28	0	0	0
11	0	0	0	.53	0	0	0	0	0	0	0	.26	0	0	0	0	0
12	0	0	0	0	0	0	0	0	0	0	0	0	.21	0	.46	0	0
13	0	0	0	0	.57	0	0	0	0	0	0	0	0	0	0	0	0
14	0	0	0	0	0	0	0	.15	0	0	0	0	0	0	0	0	0
15	0	0	0	0	0	0	0	0	0	0	0	.24	0	0	0	0	0
16	0	0	0	0	0	0	0	0	0	0	0	0	.24	0	0	0	0
17	0	0	0	0	0	0	0	0	0	0	0	0	0	.10	0	0	0

Table 5: Trend matrix V10-V1 (for explanation, see text, section 3.1 and 3.2)

	01	02	03	04	05	06	07	08	09	10	11	12	13	14	15	16	17
01	0	0	0	0	0	0	0	0	0	0	0	0	0	0	0	0	0
02	.66	0	.71	0	0	0	0	0	0	0	0	0	0	0	0	0	0
03	0	2.79	0	.13	0	0	0	0	0	0	.61	.07	0	0	0	0	0
04	0	.06	.06	0	.31	0	0	0	0	0	.32	0	0	0	0	0	0
05	0	0	0	0	0	.39	0	0	0	0	0	.67	0	0	0	0	0
06	0	0	0	0	.22	0	.03	0	.04	0	0	.05	0	0	0	0	0
07	0	0	0	0	0	.39	0	.37	.04	.05	0	0	0	0	0	0	0
08	0	0	0	0	0	0	.86	0	0	.04	0	0	.52	0	0	0	0
09	0	0	0	0	.04	.04	.13	0	0	0	0	.05	0	0	0	0	0
10	0	0	0	0	0	0	.08	1.17	0	0	0	0	.09	.25	0	0	0
11	0	.14	2.52	.74	.05	0	0	0	0	0	0	.88	0	0	.27	0	0
12	0	0	0	0	.68	.10	0	0	0	0	1.05	0	.35	0	1.28	.05	0
13	0	0	0	0	.06	0	0	.11	.14	.16	.05	.10	0	0	0	.05	0
14	0	0	0	0	0	0	0	.42	0	.07	0	0	0	0	0	0	.02
15	0	0	0	0	0	0	0	0	0	0	.48	1.64	0	0	0	0	0
16	0	0	0	0	0	0	0	0	0	0	0	0	.66	.24	.25	0	.06
17	0	0	0	0	0	0	0	0	0	0	0	0	0	.15	0	0	0

Table 6: Trend matrix C2-C1 (for explanation, see text, section 3.1 and 3.3).

	01	02	03	04	05	06	07	08	09	10	11	12	13	14	15	16	17
01	0	.22	0	0	0	0	0	0	0	0	0	0	0	0	0	0	0
02	.22	0	.50	0	0	0	0	0	0	0	0	0	0	0	0	0	0
03	0	.64	0	.27	0	0	0	0	0	0	.70	0	0	0	0	0	0
04	0	0	.07	0	.07	0	0	0	0	0	0	0	0	0	0	0	0
05	0	0	0	.08	0	.25	.04	0	0	0	0	.42	0	0	0	0	0
06	0	0	0	0	.33	0	0	0	0	0	0	0	0	0	0	0	0
07	0	0	0	0	0	.22	0	.13	.04	0	0	0	0	0	0	0	0
08	0	0	0	0	0	0	.25	0	0	0	0	0	0	0	.07	0	0
09	0	0	0	0	0	0	.04	0	0	0	0	0	0	0	0	0	0
10	0	0	0	0	0	0	0	.32	0	0	0	0	0	.04	.03	0	0
11	0	0	.56	.06	0	0	0	0	0	0	0	.64	.06	0	0	0	0
12	0	0	0	0	.42	0	0	0	.14	0	.79	0	.30	0	.40	0	0
13	0	0	0	0	.21	0	.08	0	0	0	0	.10	0	0	0	.05	0
14	0	0	0	0	0	0	0	.30	0	0	0	0	.06	0	0	0	.02
15	0	0	0	0	0	0	0	0	0	0	0	.99	0	0	0	0	0
16	0	0	0	0	0	0	0	0	0	0	0	.05	0	0	.11	0	0
17	0	0	0	0	0	0	0	0	0	0	0	0	0	0	.06	0	0

Table 7: Trend matrix S2-C2 (for explanation, see text, section 3.1 and 4)

	01	02	03	04	05	06	07	08	09	10	11	12	13	14	15	16	17
01	0	0	0	0	0	0	0	0	0	0	0	0	0	0	0	0	0
02	1.03	0	.58	0	0	0	0	0	0	0	0	0	0	0	0	0	0
03	0	1.24	0	0	0	0	0	0	0	0	.49	0	0	0	0	0	0
04	.06	.34	.67	0	0	0	0	0	0	0	.17	0	0	0	0	0	0
05	0	0	0	.92	0	.22	0	0	0	0	.20	.83	.04	0	0	0	0
06	0	0	0	0	.95	0	0	0	0	0	0	.52	0	0	0	0	0
07	0	0	0	0	.25	1.31	0	.17	0	0	0	.04	.08	0	0	0	0
08	0	0	0	0	.12	.61	2.62	0	.08	.17	0	.04	0	0	0	0	0
09	0	0	0	0	0	0	0	0	0	0	0	.18	.09	0	0	0	0
10	0	0	0	0	.10	.04	0	.59	.20	0	0	0	.12	0	0	0	0
11	0	0	1.43	.20	0	0	0	0	0	0	0	.66	0	0	0	0	0
12	0	0	0	0	.11	0	0	0	0	0	.96	0	0	0	1.05	0	0
13	0	0	0	.06	0	0	0	0	0	0	.23	.83	0	0	0	.05	0
14	0	0	0	0	0	0	0	3.58	0	.92	0	0	.05	0	0	.06	0
15	0	0	0	0	0	0	0	0	0	0	0	.92	0	0	0	0	0
16	0	0	0	0	0	0	0	0	0	0	0	.45	0	0	.34	0	0
17	0	0	0	0	0	0	0	0	0	0	0	0	0	.59	0	0	0

Table 8: Percentage land area (Antarctica excluded) covered by biomes (for numbers see Table 2) for three control runs (columns 1 - 3) and three anomaly runs (columns 4 - 6). Standard deviation of biomes from control runs (column 7) and from anomaly runs (column 8), difference between averages of columns 1 - 3 and columns 4 - 6 (column 9), and signal to noise ratio t (column 10); the hypothesis of equal averages can be rejected at a 1% significance level, if $t > 4.6, t < -4.6$, at a 5% level, if $t > 2.78, t < -2.78$

01	3.70	3.71	4.15	4.58	4.81	4.73	0.25	0.12	0.85	5.30
02	4.26	4.40	4.04	4.55	4.37	6.09	0.18	0.95	0.77	1.38
03	18.34	17.86	18.05	18.95	18.81	17.67	0.24	0.70	0.39	0.92
04	3.25	3.53	3.45	3.38	3.47	3.15	0.14	0.16	-0.08	-0.64
05	3.57	3.80	3.62	3.23	3.11	3.64	0.12	0.28	-0.34	-1.92
06	2.79	2.94	2.61	3.94	3.65	3.47	0.16	0.24	0.91	5.50
07	2.02	2.06	3.15	2.98	2.98	2.72	0.14	0.22	0.83	5.57
08	8.67	9.07	8.66	9.61	9.58	10.30	0.23	0.41	1.03	3.79
09	0.20	0.33	0.37	0.45	0.35	0.39	0.09	0.05	0.09	1.55
10	1.86	1.55	1.39	1.05	1.59	1.42	0.24	0.28	-0.25	-1.19
11	7.64	7.80	7.57	7.66	7.63	7.97	0.12	0.19	0.09	0.66
12	10.07	10.21	10.53	11.56	12.61	11.55	0.24	0.61	1.64	4.34
13	1.88	1.90	1.64	1.01	1.13	1.05	0.14	0.06	-0.75	-8.35
14	9.41	9.12	9.23	5.31	5.05	5.12	0.15	0.12	-4.08	-36.98
15	18.24	17.77	18.27	18.77	18.24	17.92	0.28	0.43	0.22	0.73
16	1.50	1.39	1.58	0.70	0.64	0.69	0.09	0.03	-0.81	-14.27
17	12.68	12.64	12.64	12.18	12.04	12.18	0.02	0.08	-0.51	-10.61

Figure 1: Allocation of colors used in Figures 2-5 and 10,11 to biomes.

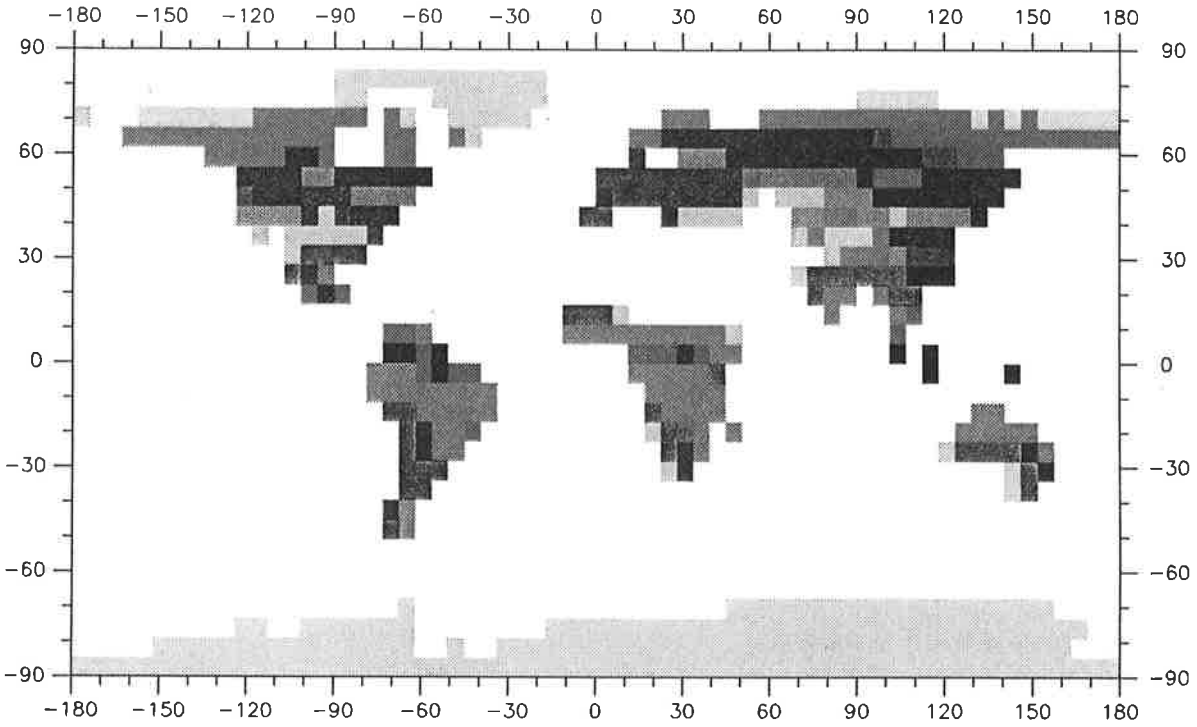

Figure 2: Present biome distributions computed from a 30-year climate simulation at T21 resolution, called T21C0.

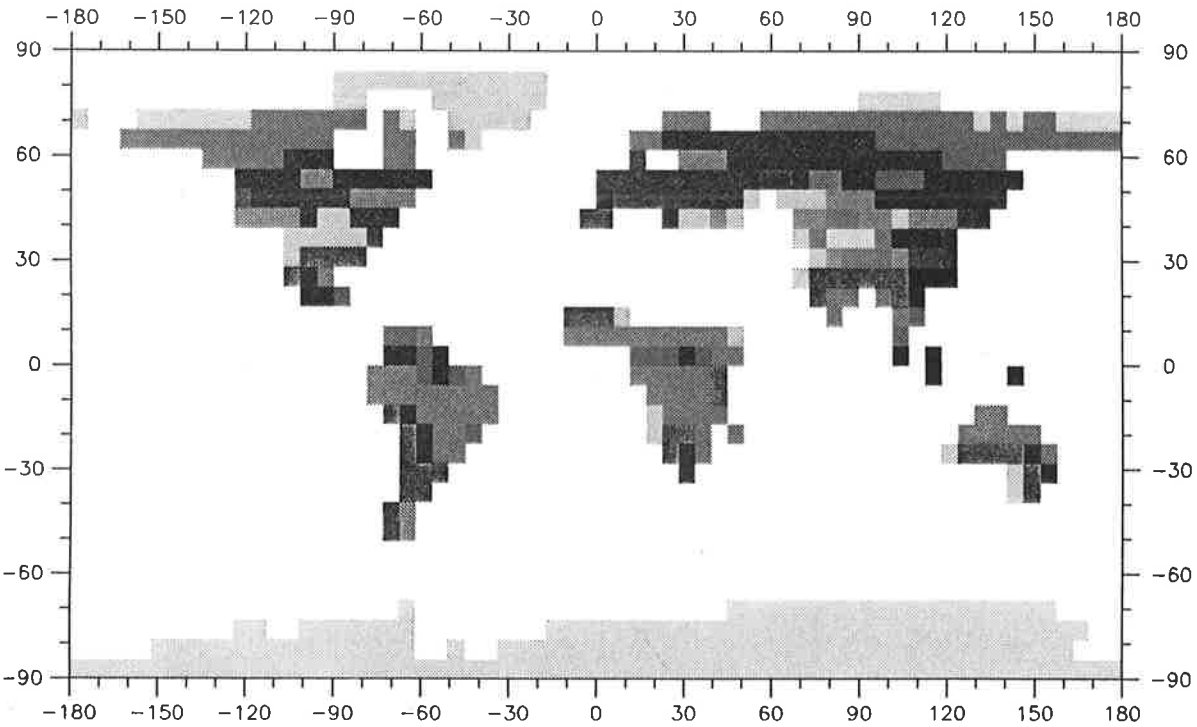

Figure 3: Same as Figure 2, but using a 10-year integration, T21C1.

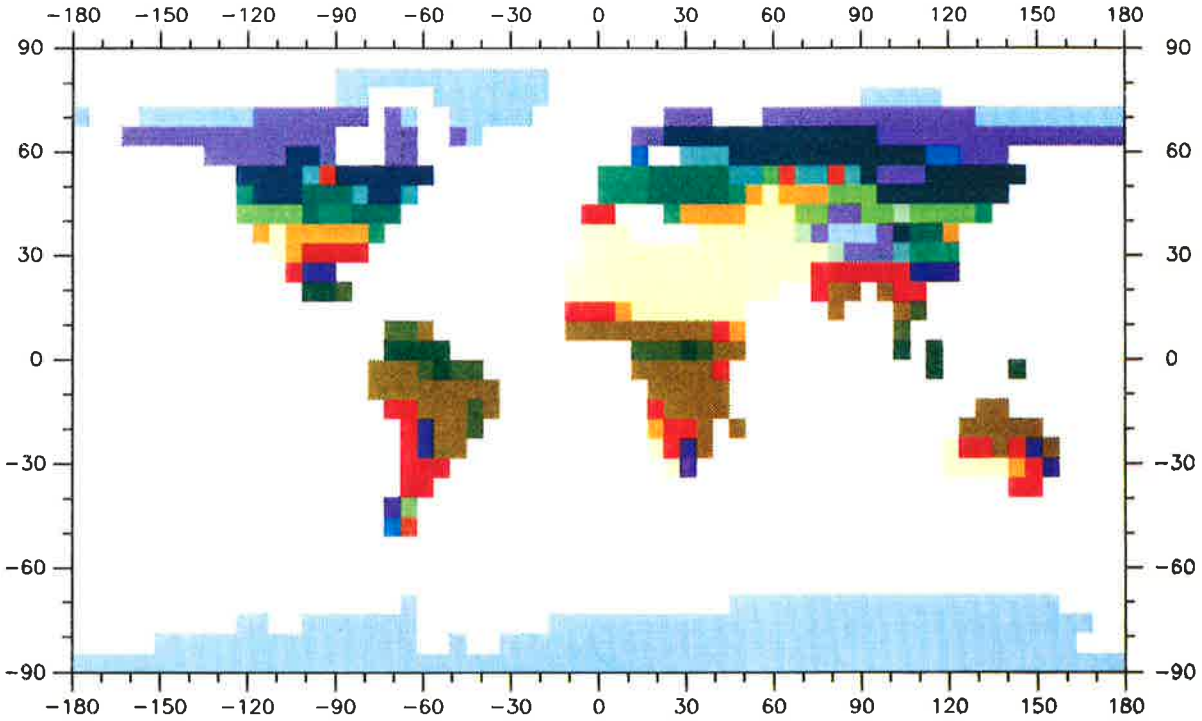

Figure 4: Same as Figure 3, but using a second 10-year integration, T21C2.

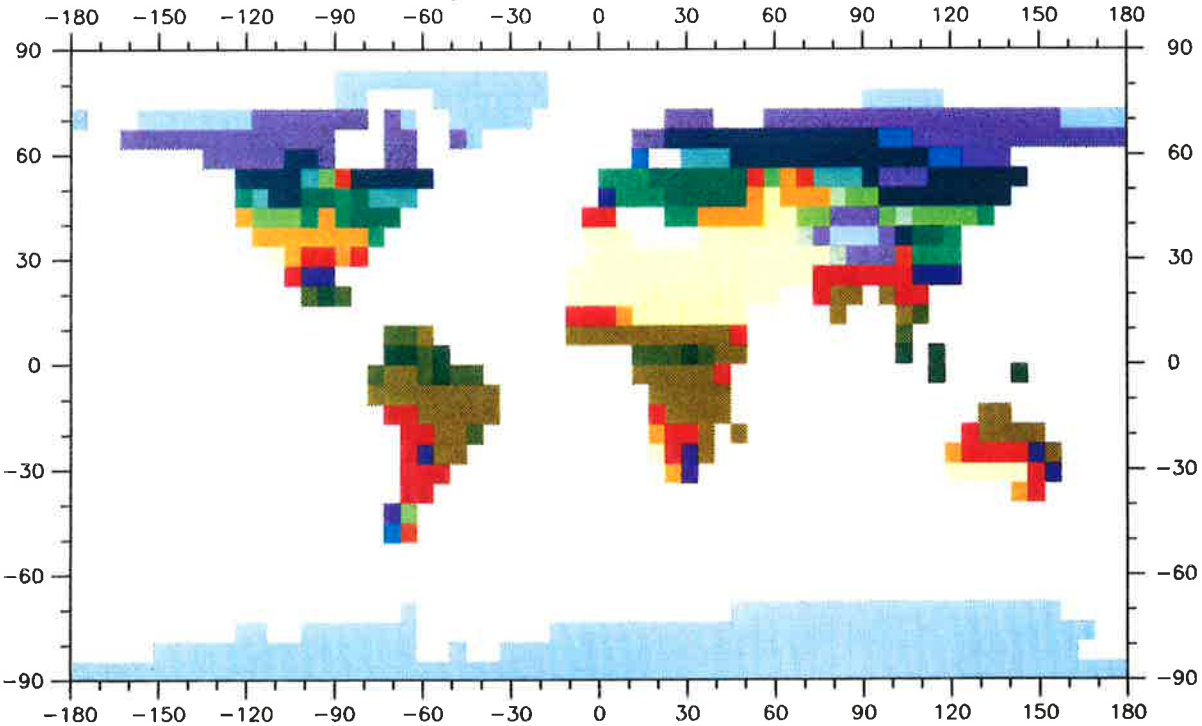

Figure 5: Same as Figure 4, but using a third 10-year integration, T21C3.

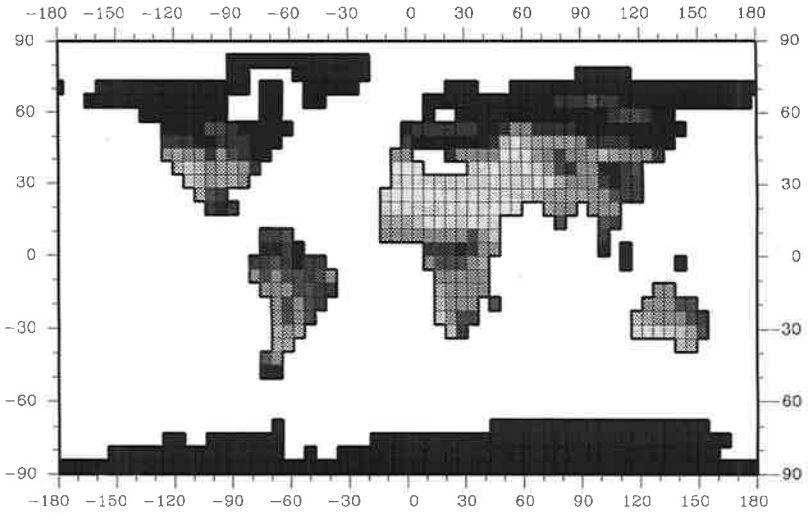

Figure 6: Global patterns of annual moisture availability evaluated from run T21C0.

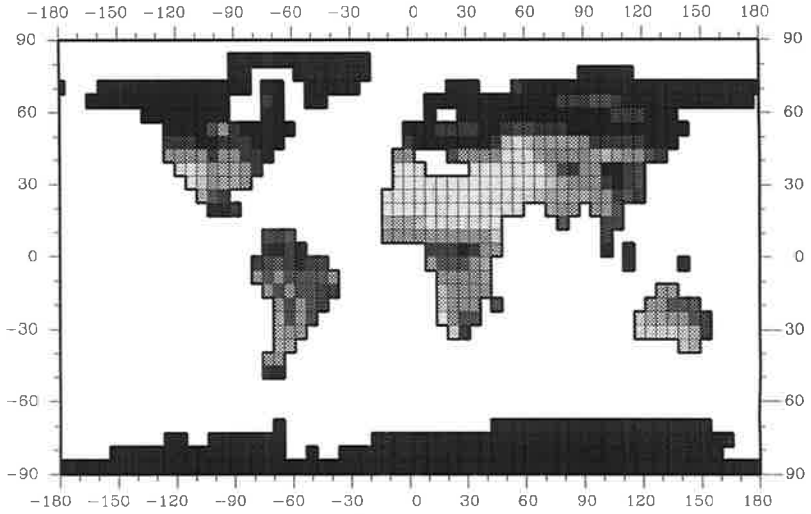

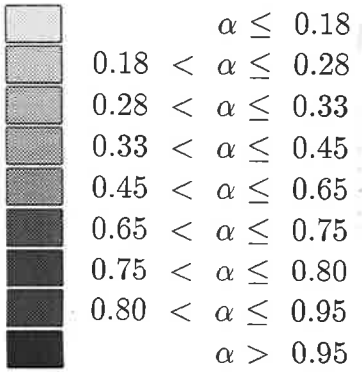

Figure 7: Global patterns of annual moisture availability evaluated from run T21C1.

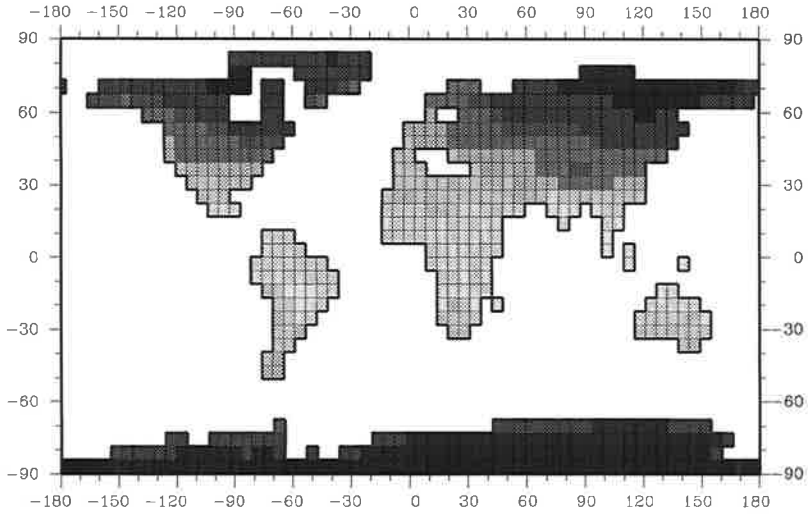

Figure 8: Global patterns of mean temperature of the coldest month evaluated from run T21C0.

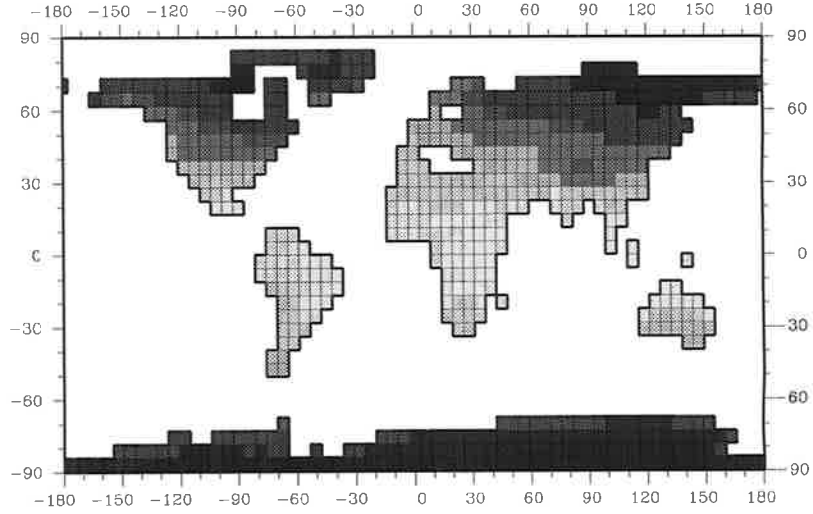

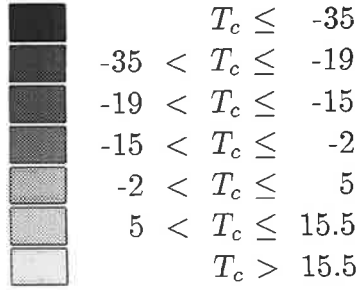

Figure 9: Global patterns of mean temperature of the coldest month evaluated from run T21C1.

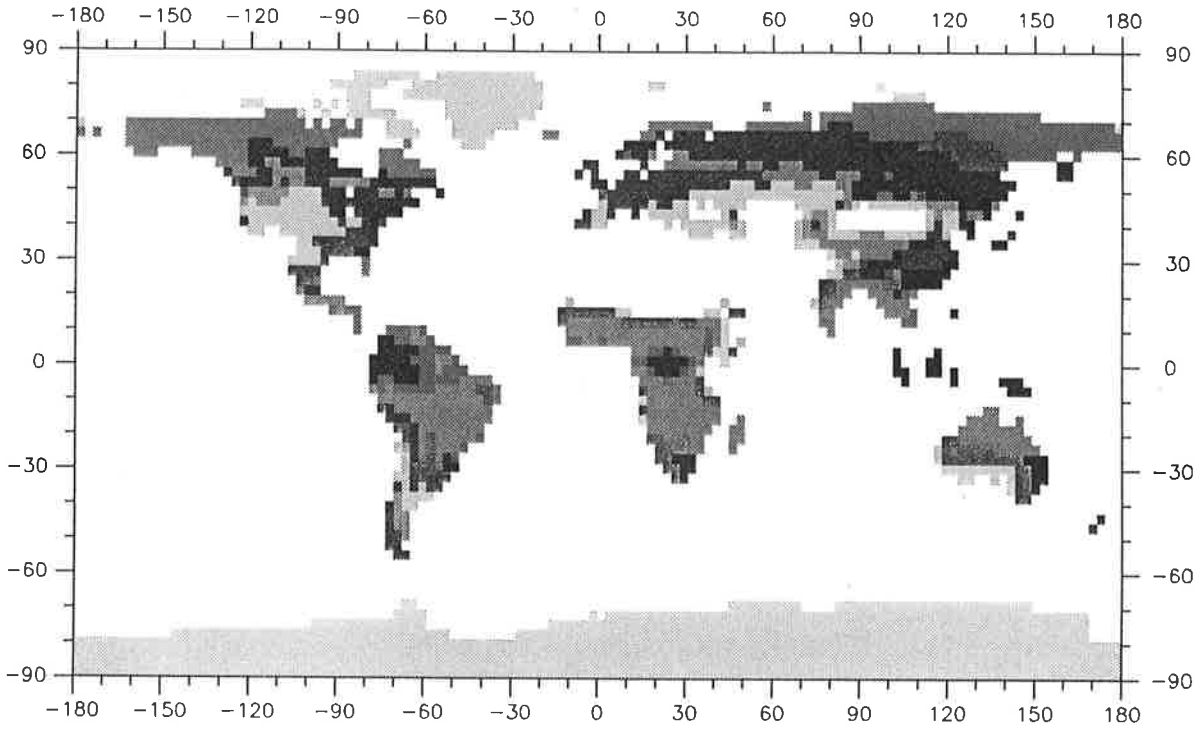

Figure 10: Biome distributions of present-day climate using a 10-year integration at T42 resolution, called C2 in the text.

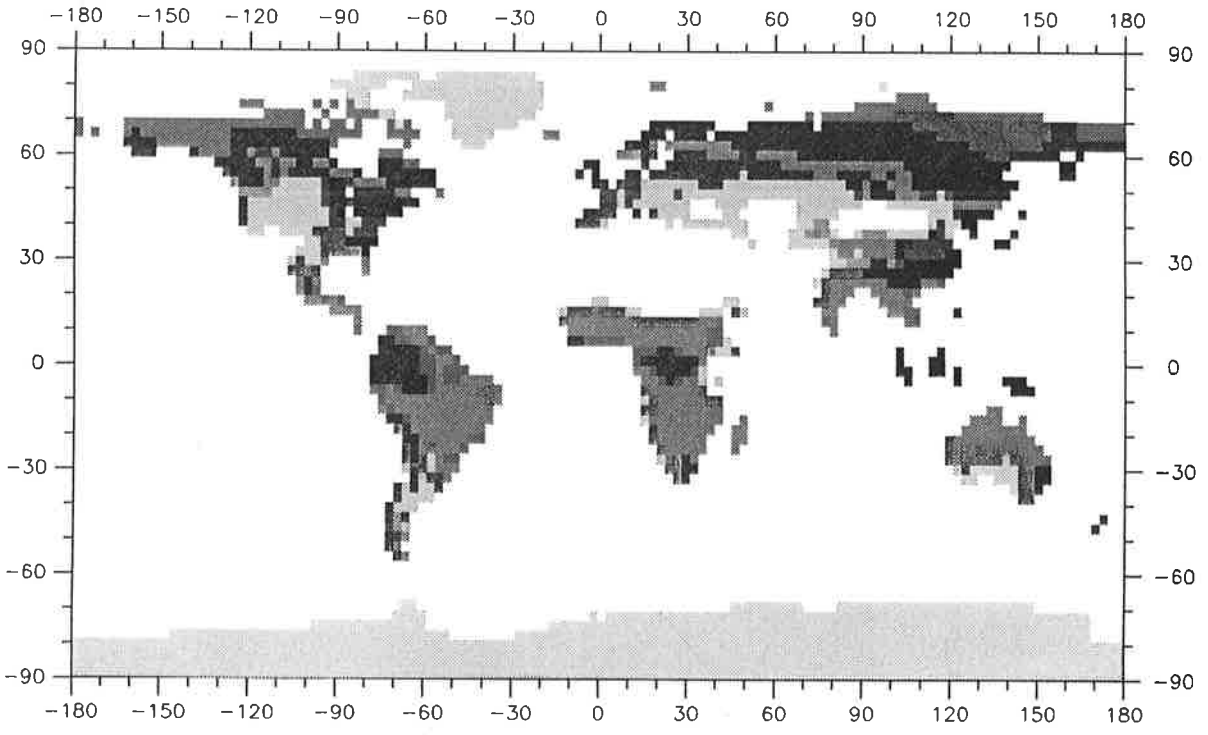

Figure 11: Change of conditions favorable for biomes due to a climate change associated with an increase of CO_2 and sea-surface temperatures computed from a climate simulation at T42 resolution, called S2 in the text.